Distribution Agreement

In presenting this thesis or dissertation as a partial fulfillment of the requirements for an advanced degree from Emory University, I hereby grant to Emory University and its agents the non-exclusive license to archive, make accessible, and display my thesis or dissertation in whole or in part in all forms of media, now or hereafter known, including display on the world wide web. I understand that I may select some access restrictions as part of the online submission of this thesis or dissertation. I retain all ownership rights to the copyright of the thesis or dissertation. I also retain the right to use in future works (such as articles or books) all or part of this thesis or dissertation.

Dehao Chen _____

4/13/2018

Date

Zoonotic Transmission Dynamics of Hemorrhagic Fever with Renal Syndrome in Urban Guangzhou, China

By

Dehao Chen
Master of Public Health

Environmental Health

Gonzalo Vazquez-Prokopec, Ph.D.
Committee Chair

Paige Tolbert, Ph.D.
Committee Member

Zoonotic Transmission Dynamics of Hemorrhagic Fever with Renal Syndrome in Urban Guangzhou, China

By

Dehao Chen

B.S.
Inner Mongolia Agricultural University
2016

Thesis Committee Chair: Gonzalo Vazquez-Prokopec, Ph.D.

An abstract of
A thesis submitted to the Faculty of the
Rollins School of Public Health of Emory University
in partial fulfillment of the requirements for the degree of
Master of Public Health
in Environmental Health
2018

Abstract

Zoonotic Transmission Dynamics of Hemorrhagic Fever with Renal Syndrome in Urban Guangzhou, China

By Dehao Chen

Background: Though Guangzhou city is not a region with a high burden of hemorrhagic fever with renal syndrome (HFRS) comparing with other areas in China, outbreaks still exist in the city due to the existence of urban rodents and a large urban population at risk. In this study, descriptive temporal analysis and geographic information system (GIS)-based spatial analysis were performed on reported HFRS cases and rodent surveys with the goal of identifying risk areas for public health interventions and ascertain the main drivers of their occurrence.

Methods: Period prevalence and the number of positive cases at different geographical scales of the city during 2008- 2016 were calculated and summarized using HFRS and rodent-borne disease surveillance data. Spatial point pattern analyses were conducted to describe global and local clustering effects of different measurements of human HFRS and rodent hantavirus at old-town and whole-city levels.

Results: Geographical distributions of HFRS cases and traps with hantavirus antibody-carrying rodents from 2008 to 2016 were mapped at the city and old-district levels in the aspect of the crude number of positive cases and period prevalence. The weighted K-function suggested that no global clustering effect existed for both the rodent and human cases in different scales of the city. Using Gi*(d) statistic, 22 significant local clusters of high infection ($P<0.05$) with different radius were discovered for the human and rodent surveillance data, and a zoonotic link was built based on the overlay of clusters of the two species. Also, we described seasonal occurrence of HFRS in the city.

Conclusion: The applications of descriptive temporal analysis, GIS and spatial point pattern analysis, offer ways to quantify zoonotic hantavirus risks across different times and spatial scales and to further recognize putative environmental determinants potentially influential in increased disease risks.

Zoonotic Transmission Dynamics of Hemorrhagic Fever with Renal Syndrome in Urban Guangzhou, China

By

Dehao Chen

B.S.
Inner Mongolia Agricultural University
2016

Thesis Committee Chair: Gonzalo Vazquez-Prokopec, Ph.D.

A thesis submitted to the Faculty of the
Rollins School of Public Health of Emory University
in partial fulfillment of the requirements for the degree of
Master of Public Health
in Environmental Health
2018

Introduction

Hemorrhagic fever with renal syndrome (HFRS) is a disease transmitted by rodents; the disease is a category of clinically similar illnesses caused by hantaviruses which belong to *Bunyaviridae* family, which includes Hantaan, Saaremaa, Dobrava, Seoul and Puumala viruses (1). HFRS is comprised of illnesses like epidemic hemorrhagic fever, nephropathia epidemica, and Korean hemorrhagic fever. HFRS is mostly distributed in Afro-Eurasia (2). There is a wide distribution of hantavirus in eastern Asia, especially in Russia, Korea and China. Dobrava virus can be found mainly in Balkans. For Puumala and Saaremaa, they are mainly endemic in western European countries, Scandinavia, and western Russia, where also have a comparatively high amount of human cases compared with the other part of Afro-Eurasia (2). There are only a few sporadic human HFRS cases reported in Southeast Asia and Africa; these interesting phenomena may be explained by the low availability of proper diagnostic testing equipment. In north and south America, hantavirus lead to a different type of illness, which is named as hantavirus pulmonary syndrome (HPS) (3). During 1999-2003, an annual average of 259 HPS in the Americas was reported, and the number of cases kept increasing in contrast to former years (4). Based on the reported data, the number of humans diagnosed with Hantavirus infection in south and north America is less than that in Afro-Eurasia continent. In Australia, no human case of hantavirus infection was reported.

There are several risk factors attributed to the transmission of hantavirus. The exposure to rodents and their excrements is the most predominant risk factor (1). Since hantaviruses are carried and spread by mice, humans are indirectly exposed to the pathogens when inhaling aerosolized urine, saliva or droppings of the infected animals. Direct exposure may also happen when contaminated urine or the other matrixes are introduced into the broken dermal layer or onto

mucous membranes (1). Also, persons working with rodents may be exposed to the pathogens when infected rodents bite them. Human to human transmission of hantaviruses is rare. Owning dogs and cats are also considered potential risk factors for hantavirus infection in humans, but the mechanisms remain unclear (5). Taking part in outdoor activities is included as another related set of risk factors globally. Research suggest that a large number hantavirus infections occur in farming operations, mediated by the relatively high abundance of rodents in farm settings. Likewise, camping and working in forests are also found to be important risk factors in European countries(6). Ecologically, meteorological changes are significant environmental determinants that influence the population density of rodents, and finally affect the disease burden in humans. For instance, due to El Nino effect, precipitation and average temperature will increase during winter, so it will be warmer in the southwestern part of the United States (7). These variations may cause higher availability of food sources for rodents in that region, and increase the number of rodents, which are associated with increased risk of HPS in the area (2).

Hantaviruses are carried by rodents, which are the natural reservoirs for the viruses. Globally, Saaremaa and Hantaan viruses are carried by *Apodemus agraius*; Soul virus is carried by *Rattus norvegicus*; Puumala virus is transmitted by *Clethrionomys glareolus*, and *Apodemus flavicollis* is the host of Dobrava virus. In China, the rodents carrying hantaviruses include *Rattus norvegicus*, *Rattus rattus*, *Rattus flavipectus, Mephitis mephitis* and *Bandicota indica.*

Clinically, the incubation period of HFRS ranges from 1 to 2 weeks after exposure to the agents. However, in rare scenarios, they may spend up to 8-week to develop clinical symptoms. Initial symptoms include back pain, abdominal pain, acute headaches, chills, and fever. Facial flushing, redness of eyes, or rash may develop during this period. Later, symptoms such as acute shock and kidney failure, vascular leakage, which can be the cause of fluid overload can appear. Depending

on the agents leading to the infection, the severity of the illness varies (8). Physicians usually make initial diagnoses of the disease based on the above symptoms. In laboratory diagnosis, immune-histochemical staining, microscope examination, and molecular biology technique are used to confirm the clinical diagnosis of HFRS.

HFRS in China accounts for nearly 90% of total HFRS cases worldwide, and the country has the most serious endemic situation around the globe (9). During 1950- 2007, there were 1,557,622 human cases and 46,427 deaths recorded (10), and 20,000-50,000 human cases were reported annually in China even though combined intervention measures including environmental regulation, control of rodents, and vaccination were implemented. The disease burden of HFRS varies highly at each administrative level across different regions of the country-127 counties in Shandong, Hubei, and Henan provinces had the most likely clusters of HFRS, where have 6.99% of the Chinese population. Most of the secondary clusters are located in the northeastern, eastern and central plain regions of the country (11).

Guangzhou city, located in the humid subtropical climate zone of southern China, is an urbanized metropolitan with high population density. Due to the conservation policy of the historic districts in the city, the older parts of the urban area went unrenovated while the suburb areas kept urbanizing and renewing. Within the old districts of Guangzhou city, a lot of infrastructures such as sewage and garbage recycle system remained old and unmaintained. In these areas, there were a lot of tenement buildings (called “Tong Lau” in Cantonese), which were designed in the way that shopkeepers could live and store goods on the upper levels of the building, and conduct commercial activities (most of the businesses belong to food catering) on the ground level. Hygiene conditions in these constructions were poor as the storage of cooking materials and waste food provided potential food sources for rodents. Also, the unrefined sewage system provided a

convenient way for the rodents to get access to diverse food sources. These environmental factors posed a potential threat for rodent-borne disease outbreaks in the old towns.

Different from traditional epidemiological methods, spatial analysis offers a better way to visualize infectious disease data and is able to account for the spatial factor that the classical linear models cannot adjust. Lots of studies were conducted to understand the spatial pattern of HFRS in various parts of China based on geographic information systems (GIS). For example, based on human surveillance data, spatial autocorrelation, inverse distance weighting interpolation, and spatial-temporal clustering analyses were used to explore the HFRS spatial patterns in Jiangsu Province (12). Based on records from the National Notifiable Disease Surveillance system and using Moran's I statistic, descriptive risk maps were plotted to indicate the annualized average incidence of HFRS in China (11). Using elliptic scanning window statistic and boosted regression trees, endemic hotspots and risk factors were indicated in Shanxi province (13).

Our study uses spatial analysis to describe the distribution pattern of HFRS in Guangzhou city across different time points with a focus on the city's old districts, and to study the geographical associations between the disease burden of HFRS in humans and hantavirus infection in rodents. As mentioned above, although studies have been conducted to understand the spreading dynamics of HFRS in China, no research was engaged to clarify the geographical pattern of the disease in the Pearl River Delta Metropolitan Region of the country, a highly dense population center with high influx of migrant workers. Also, in spite of the fact that Guangzhou is not a region with a high disease burden of HFRS, it has its particular characteristics of HFRS transmission dynamics due to high population density, humid subtropical climate, urban planning, the living habit of residents and other factors related to the transmissions of emerging infectious diseases.

Methods

Study area

The study site is located in Guangzhou city (112°57'E- 114°3'E, 22°26'N- 23°56'N), which is the capital of Guangdong province in southern China (Fig. 1). The city has a permanent population of 13,501,100 distributed in 11 districts with a total land area of 7434.40 km^2 (14). The districts of Liwan, Yuexiu and Haizhu are considered to be old areas with a population of 3,857,643 and with the sum area of 58,357 km^2 . The other districts (Tianhe, Baiyun, Huangpu, Panyu, Huadu, Nansha, Zengcheng, Conghua) are newly developed after the 1980s.

Data collection and management

HFRS is a Class B notifiable infectious disease. The diagnosis of the illness in this study used a protocol written by Chinese Center for Disease Control and Prevention (China CDC) (15). Cases were diagnosed using clinical signs and symptoms and the diagnoses were confirmed using reverse transcriptase-polymerase chain reaction (RT-PCR) or immunofluorescent antibody reaction (IFA).

Data included 2,154 human HFRS cases reported in Guangzhou during 2008-2016. The data were collected from hospitals, clinics and CDC in the 11 districts. In our study, these agencies will be considered as health care provider collectively. The records on human HFRS cases were further reported to and arranged by the division of parasitic and endemic diseases control in Guangzhou center for disease control and prevention (GZCDC), which provided the data. To calculate period prevalence, the total number of people receiving diagnostic tests in each healthcare center was recorded, this group of people is defined as the population at risk in this study. Human prevalence of HFRS was calculated as the number of individuals tested positive divided by the total number

of population at risk in the same location. Also, the number of cases in each location was summarized.

Data of rodents (covering the year 2008 to 2016) in the city was collected by local rodent control companies and CDCs in each district. This active trapping activity was led by GZCDC's rodent-borne disease surveillance project. The data of rodents were gathered by placing Sherman traps at trapping sites during nightfall, and the traps were recalled in the morning of the third day post-deployment. Trapping locations were selected by district-level CDCs; the traps were set in both indoor environments of residential areas and outdoor wild areas. For the indoor trapping in district level, 20 to 30 households were selected each month, and three to five traps were placed in each household. For the outdoor trapping at the same administrative level, the monthly trapping activities were held in farms, grasslands, ponds areas, brushwoods, forests and other rodent habitats. Although sampling bias may exist due to the subjected selection of the trapping locations, this has been reduced as much as possible. After rodents were caught, blood and lung samples were collected from the animals; IFA and RT-PCR tests were used to determine whether rodents were infected with hantavirus. The number of rodents with positive results in a trap divided by the number of rodents caught in the same trap is the period prevalence of rodents in the trap. The number of positive rodents in each trap was also recorded.

Description of spatial and temporal patterns

Histograms of annual or monthly case and prevalence were plotted to display the temporal distributions of HFRS in Guangzhou city. A district-level polygon based map at the scale of 1:50,000 were retrieved from Trimble data marketplace (16). Locations of health care providers and all traps were georeferenced by retrieving coordinates for each location, and dot maps with

district-level point layers containing these addresses were created. The number of positive humans /rodents and the number of total at-risk humans/rodents in the same location were summarized in terms of latitude and longitude. To adjust for small number problem of prevalence due to the number of population at risk at some sampling areas was small, maps of both the prevalence and the number of positive human HFRS or rodent hantavirus in different years were created. Compared with the other parts of the city, the old districts (Yuexiu, Liwan, Haizhu) had a higher population of permanent residents and more healthcare providers and restaurants; the geographical distributions of health care providers and rodent traps were more homogeneous, and the number of them was more abundant. Due to these facts, a particular emphasis was placed on these three districts using the same analyses for the whole city. The changes of prevalence and case count were indicated by graduated symbols. Since the ranges of the two disease measurements varied in different geographical scales and times, they were categorized in different ways by equal interval mode. The variance of prevalence/ the number of cases were indicated by different colors and circle sizes in maps. The disease mapping was conducted using QGIS 2.18.15 software (17), and the projection of the maps in this study was Asian Lambert Conformal Conic. The temporal distributions of HFRS were created in R language (18).

Point pattern analysis

Point pattern analysis is a study of spatial arrangement of points in a geographical area (19). In this study, the analysis was used to identify whether aggregations of more than the expected number of disease measurements of human HFRS cases and rodent hantavirus existed in the two scales of the city, and clustering tests based on the software program Point Pattern Analysis (PPA)

(20) was used to calculate a global spatial statistic- the weighted-K function, and the local spatial statistic- the Gi*(d).

Spatial statistics is computed by giving differential weight to the distances between events of interest (21). The weighted-K function utilizes a Euclidean distance matrix of every distances among points for analyzing the spatial distribution patterns of measurements of values (case count and prevalence) among all places (rodent traps and healthcare providers). The analysis is conducted in rectangular areas, which are created based on the magnitude of the study area, the number of points (e.g., health care providers, traps), distances among points, and the value of each point (e.g., case count, prevalence). Compared with a confidence interval generated based on independent and random allocations of observed values to the defined locations for an identified number of Monte Carlo Simulations, the P value for whether the observed pattern distributes randomly is determined. In this study, the weighted-K function was used to determine whether global clustering existed in the city and old-district levels. The Gi*(d) local test is used to quantify clustering of weighted events at the local level, and it is able to identify hot spots via comparing the value of a given point to all other values within specified searching distances without including the point of focus. Due to the existence of multiple comparisons in the test, an adjusted significant level is determined (22). In this study, Gi*(d) was used to assess local clustering of the two measurements of infection of hantavirus in the two species and different geographical scales of the city.

For weighted-K and Gi*(d) statistics used in this study, different parameters were used in different scales. As the analysis in the whole-city level, the maximum search radius was defined as 20, 000 m and 50 was chosen as the number of increment. 5,000 m and 50 times were selected as the maximum search radius and increments respectively for the analysis in the old-district level.

The above searching distances and increments were set as parameters for both the weight-K and Gi*(d) statistics. The selection of the above parameters was based on the geographical shape of the city and allocations of healthcare resources and rodent traps (Fig. 2, Fig. 3). For weight-K function, 999 was set as the number of Monte Carlo permutations for creating the confidence interval.

Results

Allocation of traps and healthcare resources

From 2008 to 2016, the geographic distribution of rodent traps indicated that among the 123 traps placed throughout the city, 70 (56.91%) of the traps were located in the three old districts (Fig. 3). The placements of traps in the other parts of the city were relatively sparse. In the peripheral areas of the city such as Conghua and Nansha districts, there were only two traps being placed. The distribution of healthcare providers was similar to the allocation of traps (Fig. 2, Fig. 3)- most of the healthcare facilities were located in the old districts and southwest part of Tianhe district. These districts were located in the Midwestern part of the city. The farther the distance from this part of the city, the less the healthcare facilities that conducted HFRS examinations existed.

Descriptive temporal and spatial analyses

At the city level, there were 17, 314 patients who received the HFRS diagnostic tests from 2008 to 2016; this group of people was considered as the population at risk in this study. Among the individuals who received the examinations of HFRS, 2,154 persons tested positive (12.44%). The period prevalence during the whole study duration was 12.44%. From 2008 to 2011, the annual

prevalence increased from 9.33% to 17.92% (Fig.4). After peaking in 2011, the annual prevalence presented a decreasing trend until the end of the period of analysis (2016) (Fig. 4). For the change of cases across different years, the unimodal trend peaked in 2014 and decreased thereafter (Fig. 5). Within years, a seasonality trend can be observed that one peak occurred in spring and kept decreasing until the third quarter of the year; after that, the other peak appeared in winter (Fig. 6).

At the old-district level, 11,229 persons were tested for HFRS infection during the entire study period and 1,322 (11.77%) of them tested positive. The population received the tests in the three old districts accounted for 64.86% of the population received the tests in the whole city. Due to the fact that the sample size in the old districts yielded a higher statistical power, and the areas owned a more critical hygienic status as mentioned before; same analyses were conducted specifically for this region. The changing trends of annual prevalence and cases of human HFRS in the old towns (Fig. 6, Fig. 7) were similar to the ones in the whole city (Fig. 4, Fig. 5).

Human HFRS distribution based on the location of health care providers indicated that cases were mainly located in the Midwestern part of the city, and fewer cases were located in the outer and more rural parts of the city (Fig. 8, Fig. 10). All districts in Guangzhou city reported human HFRS cases over the nine-year study (Fig. 8, Fig. 10). Four districts located in the metro area had a higher prevalence across different years (Fig. 8). The distributions and prevalence of cases in the peripheral part of the city varied by year. The four districts with the highest prevalence during the 9-year period were Yuexiu, Liwan and Haizhu, which were analyzed together as old districts due to the similarity of urban structure among them, and the fourth district is Tianhe district, which was newly developed after the 1990s. The old districts had a total prevalence of 11.78% and Tianhe district had a prevalence of 14.06% across the nine-year study period. For the measurement of

disease burden using the number of cases in each location (Fig. 9, Fig. 11), the results were identical to the ones using prevalence (Fig. 8, Fig. 10).

A total of 6,090 rodents were caught during the entire study period in 123 traps across the city, with 643 of them testing positive for hantavirus antibodies (10.56%); Hantavirus infection prevalence in rodents was similar to the aggregated prevalence in human for the same period. Because the locations of rodent survey were selected by various rodent control companies under the supervisions of district-level CDCs, the spatial distributions of traps in different years were different, since different companies had different preferences of selecting trapping locations. Owing to this scenario, the analysis on rodent surveillance data was treated in a cross-sectional way to yield a more widespread distribution of traps and larger sample size. Similar to the scenario in human, a number of surveyed rodents with positive testing results were located in the mid-western part of the city (Fig. 13, Fig. 14). All districts except Huadu detected rodents carrying hantavirus antibodies over the whole study period. In the off-lying districts, it should be noticed that Zengcheng and Baiyun districts also detected the existence of hantavirus antibody in six and five traps, respectively (Fig. 12, Fig. 13).

Point pattern analysis

Within the two scales, weighted K-function revealed the two measurements at locations of both healthcare providers and rodent traps were randomly distributed within the pattern of points, which indicated that global spatial clustering didn't exist (Fig. 15).

For the analyses of local clustering, Gi*(d) statistics identified 22 clusters in different scales of the city, testing species and measurements of diseases. For the analysis of the healthcare providers in the whole city using the number of positive cases in each location as measurement, there were

nine significant local clusters located in the eastern part of Yuexiu district, the southwestern part of Tianhe district and the eastern part of Haizhu district (Fig.16). The six clusters in Yuexiu district were so closed that they dissolved together. In these hot spots of Yuexiu district, five of them had a radius of 800 m and one of them had a radius of 100 m (Fig. 16). In Tianhe district, the two clusters with the same radius of 400 m were also proximal to each other (Fig. 16). The cluster detected in Haizhu districts had a radius of 3,200 m, which also covered nearby Tianhe, Huangpu and Panyu districts (Fig. 16). In the whole city scale, for the analysis of rodent traps performed using the same measurement, two overlaid clusters with the same radius of 2000 m were discovered in southern part of Baiyun district which shared borders with Yuexiu district (Fig. 18). Another cluster with a radius of 4,000 m was detected in southern Tianhe district (Fig. 18). Interestingly, this cluster intersected the cluster of the healthcare provider in Haizhu district, which built up a zoonotic link of rodent hantavirus infection and human HFRS (Fig. 23).

In the city-wide scale, two significant clusters of high human infection prevalence with the same radius of 400 m were located in southwestern Tianhe district (Fig. 17). No cluster existed for the rodent prevalence data. In Tianhe district, the location of the clusters intersected with the ones calculated for the number of positive cases (Fig. 16, Fig. 17).

When the same local analysis was conducted for the old districts using the number of positive cases, two clusters with radiuses of 400 m and 5000 m were found in the mid-eastern part of Yuexiu district and eastern part of Haizhu district, respectively (Fig. 20, Fig. 27). For this two clusters, it should be noticed that they overlaid with the result in the scale of the whole city using the same measurement (Fig. 16, Fig. 20). As the analysis for the positive case count of rodent trap data in these three districts, three dissolved clusters located in the central part of Liwan district were found proximal to each other, they had radiuses of 3600 m, 3100 m, and 2900 m (Fig. 21,

Fig. 27). Compared with the area of Liwan district, the total area of the three clusters was relatively large in this old town, this suggested that Liwan district had a higher number of rodents carrying hantavirus comparing with other two old towns.

In the scale of old districts, the clusters generated using prevalence data from healthcare providers and rodent traps were generally smaller in area than the other clusters mentioned before (Fig. 23, Fig. 27). Two clusters existed for the spatial clustering in healthcare resources, one was located in the mid-western part of Yuexiu district, and it had a radius of 100 m; the other one was positioned in the mid-eastern part of Liwan district, which also covered the western part of Haizhu district (Fig. 19). Only one cluster was found for the prevalence of rodent traps, it was located in the mid-northern part of Yuexiu district and had a radius of 400 m (Fig. 22).

Discussion

In this study, descriptive spatial and temporal analyses and statistical point pattern analyses of Human HFRS and rodent hantavirus were conducted at the district level of Guangzhou city at different spatial scales. Our analyses pinpointed geographical areas with significant high number of human HFRS and rodent hantavirus in Guangzhou; making possible a geographical zoonotic connection between the disease hotspots in humans and rodents.

The mapping of traps and healthcare resources revealed that the Mid-western part of the city had the highest burden of HFRS and hantavirus. It is known that the distribution of hantaviruses in humans and rodents are associated with the geographical location of socio-economic status (SES) and human population density. This can be explained by the fact that individuals with lower SES tend to live in the areas with poor hygiene, which increase their potential of exposure to rodents (23). The places with high population density store more food and produce more waste, which

promote the population growth of rodents (10, 23, 24). Urban Guangzhou owns highly heterogeneous distribution of these two drivers (25). Hence, the two anthropological factors should be considered when interpreting the distributions of human HFRS and rodent hantavirus. Furthermore, the array of non-anthropological factors that led to disease clusters is multifaceted. In the metro areas that rodent and human clusters are located (Fig. 25, Fig. 26), it can be seen that the clustering effects are overlaid with multiple environmental factors such as high density of buildings, close proximity to water, variance of greenspace, elevation, land use and the other factors they may explain the occurrence of human HFRS and rodent hantavirus. Similar determinants were also observed in other studies understanding the epidemiology of zoonotic hantavirus. For instance, artificial (human-made) areas, cropland, elevation were found associated with the increase risk of HFRS in Shanxi province, China (13). Landscape elements like normalized difference vegetation index (NDVI), elevation, and appearance of forests were remarkably associated with HFRS in China (26). Besides, meteorological factors also determine the appearance of HFRS cases. By observation, there were two peaks for the annual temporal distribution of HFRS, which can be described as a bimodal distribution (Fig. 6). The causes for the spring and winter peaks and the variation of the number of cases in different years may be explained by the relatively low temperature, high humidity and low precipitation in the two seasons. These elements create a better environment for the survival of hantavirus and increase the probability of human exposure to the pathogen. Similar patterns were found in other areas (27, 28). In China, HFRS cases peaked twice in spring and winter from 2006 to 2010, the spring peak was lower and broader and the winter peak was higher and narrower (27). During 1992 to 2014, high number of HFRS appeared in former months (January-March) of the years and the last three months of the years (29). Except for the above factors causing occurrence of HFRS, the spatial

distributions and temporal changes of the disease can also be influenced by the reproduction and activities of rodents, and viral types (30, 31).

The surveillance of hantavirus in rodents and humans was based on "the surveillance protocol of HFRS for Guangzhou city" (32), the distributions of traps were similar to the locations of hospital resources. This implied that the implementation of the surveillance policy varied by districts- the districts in the Midwestern urban area implemented the rodent survey better than the outlying districts due to the outlying areas owned less funding resources. Thus, the maps developed in this work provide information for future allocation of rodent trapping surveys in the whole city and offer insights for public health planning and allocation of healthcare resources.

In our research, global and local spatial statistics were implemented to qualify whether clustering existed in the weighted locations and quantify the extent of clusters by prevalence and number of positive cases. While global weighted-K statistics do not identify particular clusters, local Gi*(d) statistic allows detection of specific locations of clusters for high values of measurement (33). The spatial distribution of rodent hantavirus and HFRS in Guangzhou city were nonrandom and clustered locally with different radiuses, up to 5,000 m. The areas and locations of the zoonotic clustering patterns varied by the scales of the study. However, it should be noticed that the spatial differences between the hotspots generated by the two measurements were more likely caused by the "small number problem"(34). In this study, prevalence was calculated by dividing the number of humans or rodents detected with positive hantavirus testing results by the number of humans or rodents received the test. The variance of prevalence relies heavily on the magnitude of the denominator. In the data collection steps, selection bias existed since the local-level healthcare workers were more likely to provide examinations for people presented the clinical syndromes and trap rodents from higher risk areas based on *a priori* knowledge. The variance of

prevalence was high and sometimes the prevalence was equaled to one due to no negative result was collected, and the unbiased underlying prevalence might be totally unremarkable. This is also a common problem for similar researches using infectious disease surveillance data (35)- unlike classical epidemiological studies which usually include control groups, infectious disease surveillance usually gathers information from individuals with diseases so that sometimes it is not proper to calculate measurements of disease frequency such as incidence and prevalence.

We identified clusters of hantavirus in rodent and humans and discovered the geographical zoonotic overlay of this two types of hotspots located in the eastern border of Tianhe and Haizhu districts (Fig. 23, Fig. 26). In the hotspots in which HFRS and rodent hantavirus burden are high, focusing on prevention strategies at these regions of high risk can optimize the effectiveness of health maintenance program of the city and break the zoonotic link of hantavirus transmission. Individuals living in hotspot areas should be informed of the potential of infection and be given advise on prevention methods. Our study is the first in China that utilized both human surveillance and rodent survey information to conduct point pattern analysis and discovered the spatial zoonotic overlay of the two forms of hantavirus infection across species.

Conclusions and Recommendations

This study described the temporal pattern and investigated the spatial distribution of human HFRS and rodent hantavirus in Guangzhou city, China, during 2008 to 2016 using existing surveillance data, GIS, and spatial statistics. PPA identified clusters in central and central-west parts of the city and found the zoonotic connection between the rodent and human clusters, which have not been reported previously. The data also provided evidence that the occurrence of HFRS followed a seasonal trend. These findings offered information for the allocation of medical and

public health resources in preventing the disease in human and eliminate the pathogen in urban rodents, and also lay a foundation to conduct further research in the environmental determinants in the urban settings responsible for the increase of zoonotic transmission risk.

Bibliography

1. CDC. Hemorrhagic Fever with Renal Syndrome (HFRS) 2017 [cited 2018 March 26]. Available from: https://www.cdc.gov/hantavirus/hfrs/index.html.
2. Watson DC, Sargianou M, Papa A, Chra P, Starakis I, Panos G. Epidemiology of Hantavirus infections in humans: A comprehensive, global overview. Critical reviews in microbiology. 2014;40(3):261-72.
3. CDC. Hantavirus Pulmonary Syndrome (HPS) 2013 [cited 2018 March 25]. Available from: https://www.cdc.gov/hantavirus/hps/index.html.
4. PAHO. Case development of Hantavirus Pulmonary Syndrome (HPS) (Region of the Americas, by country and year, 1993-2002) 2003 [Available from: http:// www.paho.org/common/Display.asp?Lang¼E&RecID¼6044.
5. Ruo SL, Li YL, Tong Z, Ma QR, Liu ZL, Tang YW, et al. Retrospective and prospective studies of hemorrhagic fever with renal syndrome in rural China. J Infect Dis. 1994;170(3):527-34.
6. Crowcroft N, Infuso A, Ilef D, Le Guenno B, Desenclos J, Van Loock F, et al. Risk factors for human hantavirus infection: Franco-Belgian collaborative case-control study during 1995-6 epidemic. Bmj. 1999;318(7200):1737-8.
7. Kovats RS, Bouma MJ, Hajat S, Worrall E, Haines A. El Niño and health. The Lancet. 2003;362(9394):1481-9.
8. Linderholm M, Elgh F. Clinical characteristics of hantavirus infections on the Eurasian continent. Hantaviruses: Springer; 2001. p. 135-51.
9. Bai X, Huang C. Study farther on hemorrhagic fever with renal syndrome. Chin J Infect Dis. 2002;20:197-8.
10. Zhang YZ, Zou Y, Fu ZF, Plyusnin A. Hantavirus infections in humans and animals, China. Emerg Infect Dis. 2010;16(8):1195-203.
11. Fang L, Yan L, Liang S, de Vlas SJ, Feng D, Han X, et al. Spatial analysis of hemorrhagic fever with renal syndrome in China. BMC Infect Dis. 2006;6:77.
12. Bao C, Liu W, Zhu Y, Liu W, Hu J, Liang Q, et al. The spatial analysis on hemorrhagic fever with renal syndrome in Jiangsu province, China based on geographic information system. PloS one. 2014;9(9):e83848.
13. Liang W, Gu X, Li X, Zhang K, Wu K, Pang M, et al. Mapping the epidemic changes and risks of hemorrhagic fever with renal syndrome in Shaanxi Province, China, 2005–2016. Scientific reports. 2018;8(1):749.
14. Guangzhou Statistics Bureau. Information of administrative districts in Guangzhou 2016 [Available from: http://www.gzstats.gov.cn/gzsq/200812/t20081230_430.html.

15. CCDC. Diagnosis standard 2005 [Available from: http://www.chinacdc.cn/jkzt/crb/lxxcxr/cxrzstd/200506/t20050629_24193.htm.
16. Trimble Data Marketplace. Guangzhou city map 2017 [Available from: https://market.trimbledata.com/ - /search?east=-80.35282314453127&north=35.68642110660353&south=31.847356398724486&west=-88.34537685546876&zoom=8.
17. QGIS Development Team. QGIS Geographic Information System. 2017. p. Open Source Geospatial Foundation Project.
18. R Core Team. R: A Language and Environment for Statistical Computing. 3.4.3 ed2018.
19. Gatrell AC, Bailey TC, Diggle PJ, Rowlingson BS. Spatial Point Pattern Analysis and Its Application in Geographical Epidemiology. Transactions of the Institute of British Geographers. 1996;21(1):256-74.
20. Dongmei Chen AG. Point Pattern Analysis. San Diego, CA1998.
21. Kitron U. Landscape ecology and epidemiology of vector-borne diseases: tools for spatial analysis. Journal of medical entomology. 1998;35(4):435-45.
22. Ord JK, Getis A. Local spatial autocorrelation statistics: distributional issues and an application. Geographical analysis. 1995;27(4):286-306.
23. Kallio ER, Begon M, Henttonen H, Koskela E, Mappes T, Vaheri A, et al. Cyclic hantavirus epidemics in humans—predicted by rodent host dynamics. Epidemics. 2009;1(2):101-7.
24. Olsson GE, Dalerum F, Hörnfeldt B, Elgh F, Palo TR, Juto P, et al. Human hantavirus infections, Sweden. Emerging Infectious Diseases. 2003;9(11):1395.
25. Yeh AG-O, Xu X, Hu H. The social space of Guangzhou city, China. Urban Geography. 1995;16(7):595-621.
26. Yan L, Fang L-Q, Huang H-G, Zhang L-Q, Feng D, Zhao W-J, et al. Landscape elements and Hantaan virus–related hemorrhagic fever with renal syndrome, People's Republic of China. Emerging infectious diseases. 2007;13(9):1301.
27. Huang X. Epidemiologic characteristics of haemorrhagic fever with renal syndrome in Mainland China from 2006 to 2010. 2012.
28. Tian H-Y, Yu P-B, Luis AD, Bi P, Cazelles B, Laine M, et al. Changes in rodent abundance and weather conditions potentially drive hemorrhagic fever with renal syndrome outbreaks in Xi'an, China, 2005–2012. PLoS neglected tropical diseases. 2015;9(3):e0003530.
29. Li S, Cao W, Ren H, Lu L, Zhuang D, Liu Q. Time Series Analysis of Hemorrhagic Fever with Renal Syndrome: A Case Study in Jiaonan County, China. PloS one. 2016;11(10):e0163771.
30. Zhang Y-Z, Zhang F-X, Gao N, Wang J-B, Zhao Z-W, Li M-H, et al. Hantaviruses in rodents and humans, Inner Mongolia Autonomous Region, China. Emerging infectious diseases. 2009;15(6):885.
31. Chen H-X, Qiu F-X, Dong B-J, Ji S-Z, Li Y-T, Wang Y, et al. Epidemiological studies on hemorrhagic fever with renal syndrome in China. Journal of Infectious Diseases. 1986;154(3):394-8.
32. GZCDC. The surveillance protocol of HFRS for Guangzhou city. In: diseases Doeap, editor. 2017.
33. Anselin L. Local indicators of spatial association—LISA. Geographical analysis. 1995;27(2):93-115.

34. Jazquez G. The small numbers problem: What you see is not necessarily what you get. 2010 [Available from: https://www.biomedware.com/blog/2010/small_numbers_problem1/.
35. Lin H, Liu Q, Guo J, Zhang J, Wang J, Chen H. Analysis of the geographic distribution of HFRS in Liaoning Province between 2000 and 2005. BMC public health. 2007;7(1):207.

Tables & Figures

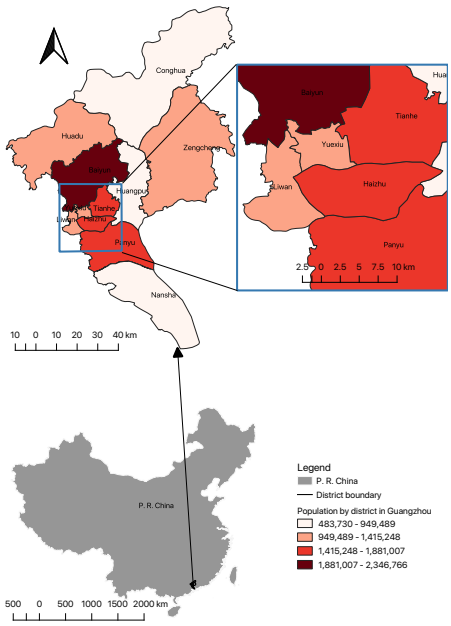

Figure 1. Population distribution in Guangzhou city by district. Inset shows the population distribution within the old town districts.

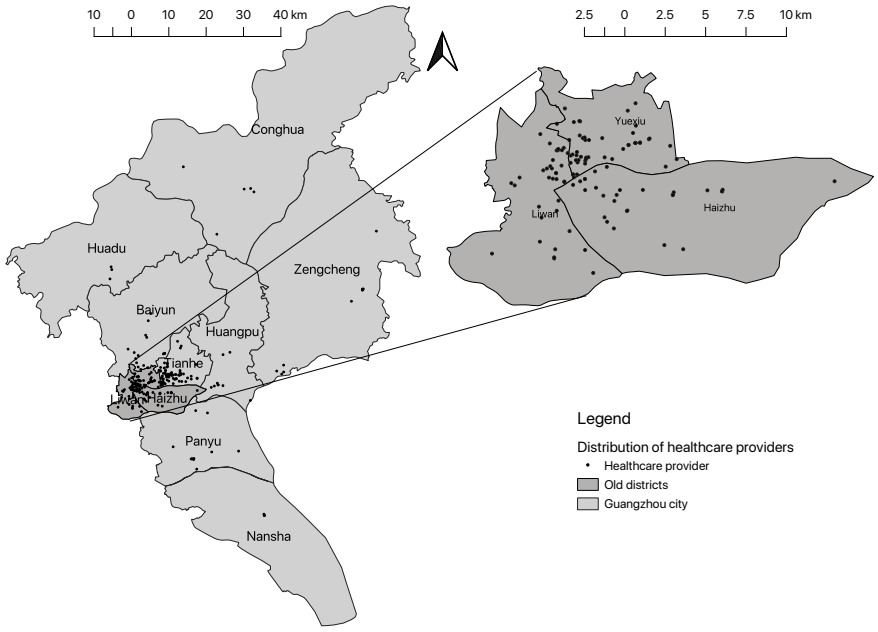

Figure 2. Distribution of healthcare providers in Guangzhou city (2008-2016). Inset shows the location of points within the old town.

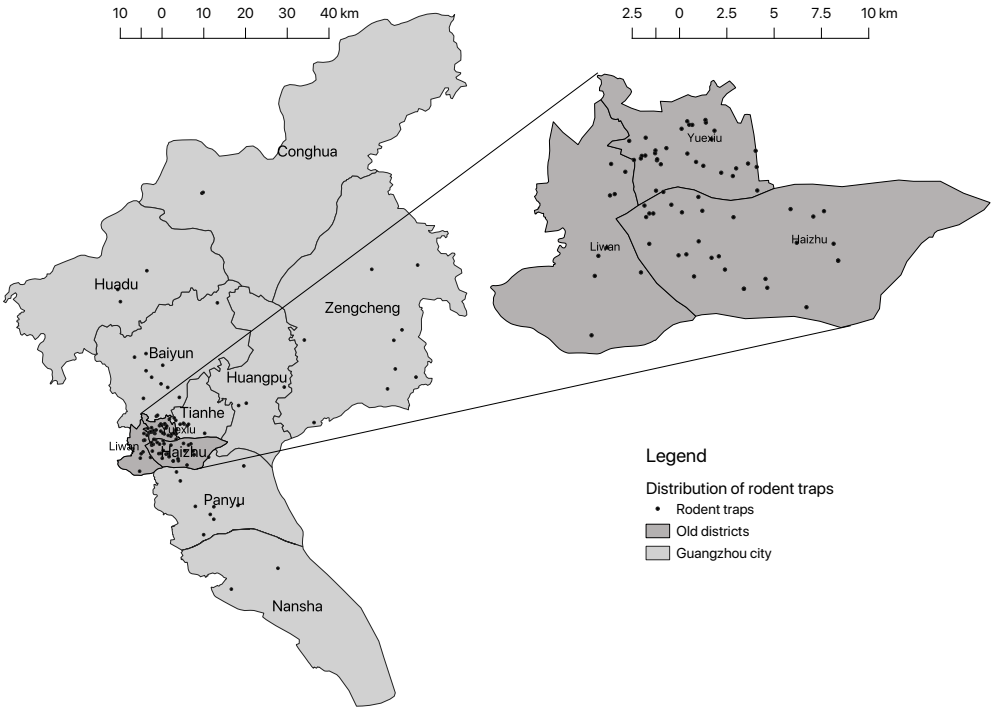

Figure 3. Distribution of rodent traps in Guangzhou city (2008-2016). Inset shows the location of points within the old town.

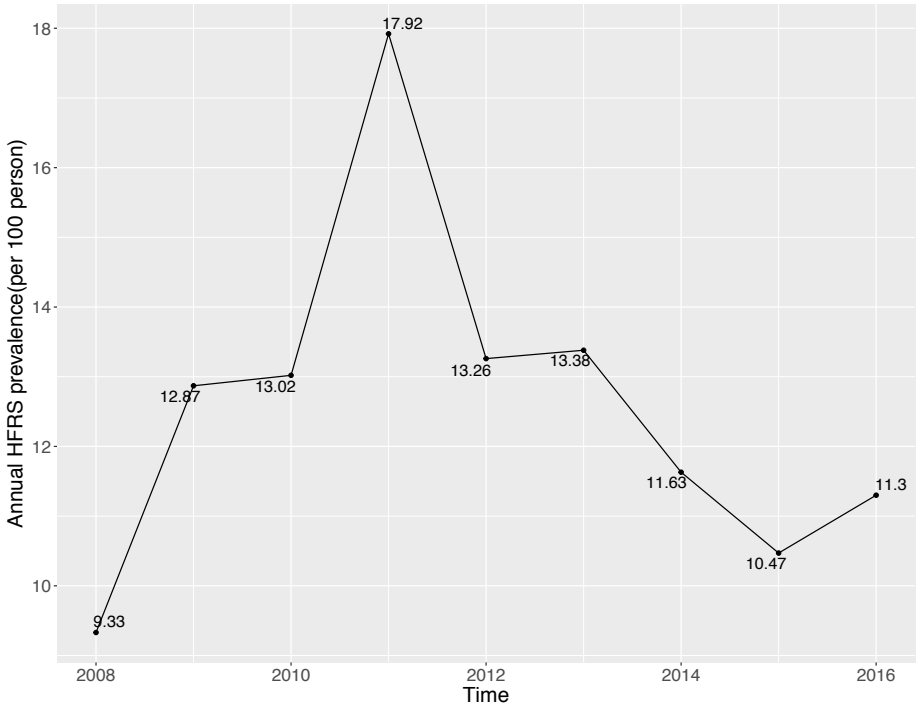

Figure 4. Temporal distribution of human HFRS prevalence in Guangzhou city, 2018-2016

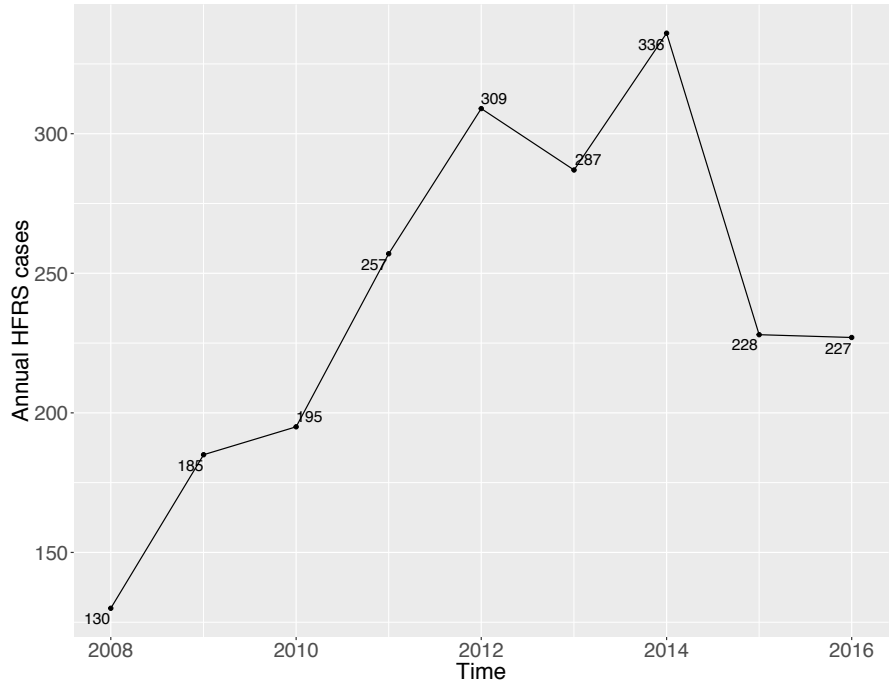

Figure 5. Temporal distribution of human HFRS cases in Guangzhou city, 2008-2016.

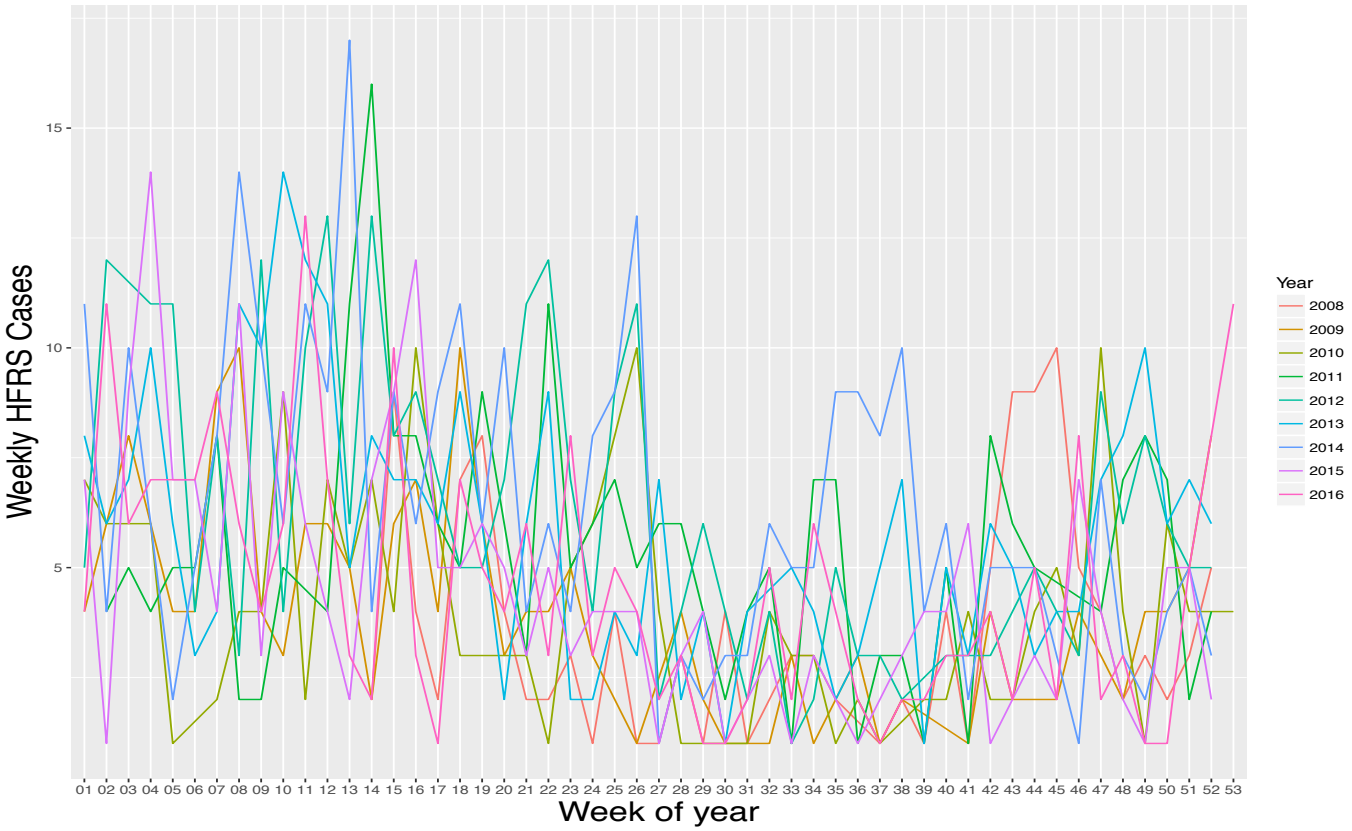

Figure 6. Temporal distribution of human HFRS cases in Guangzhou city by week, 2008-2016.

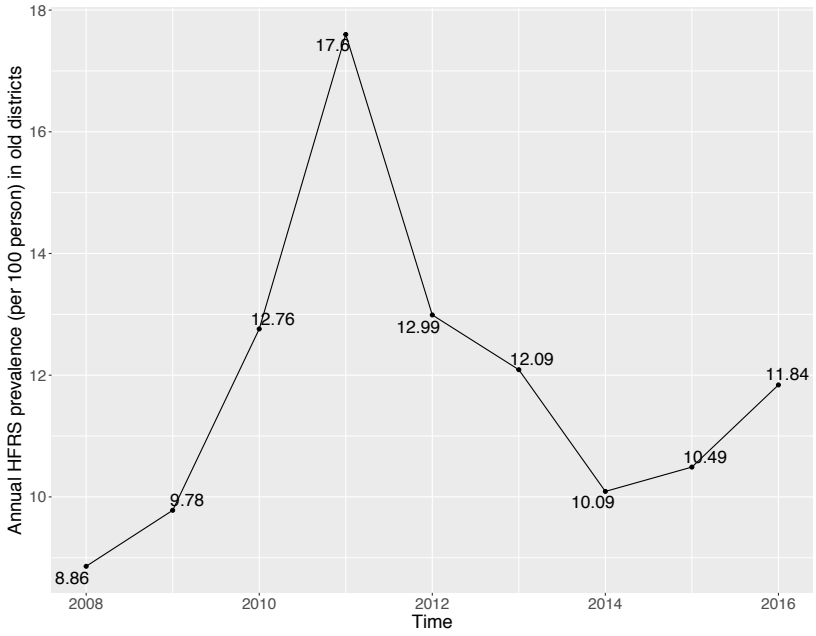

Figure 7. Temporal distribution of human HFRS prevalence in old districts, 2008-2016.

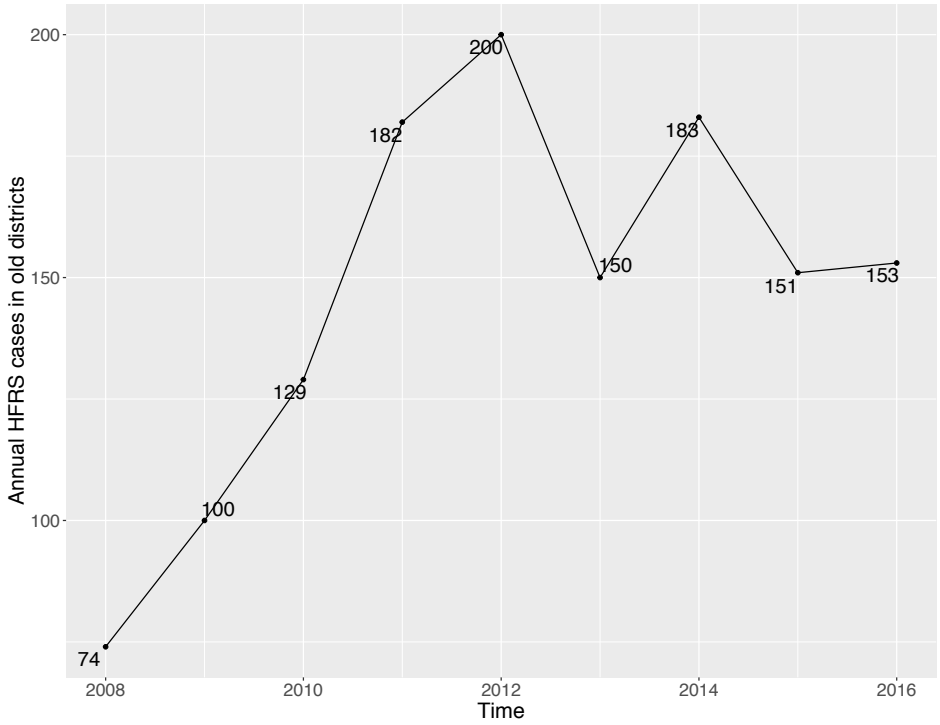

Figure 8. Temporal distribution of human HFRS cases in old districts, 2008-2016.

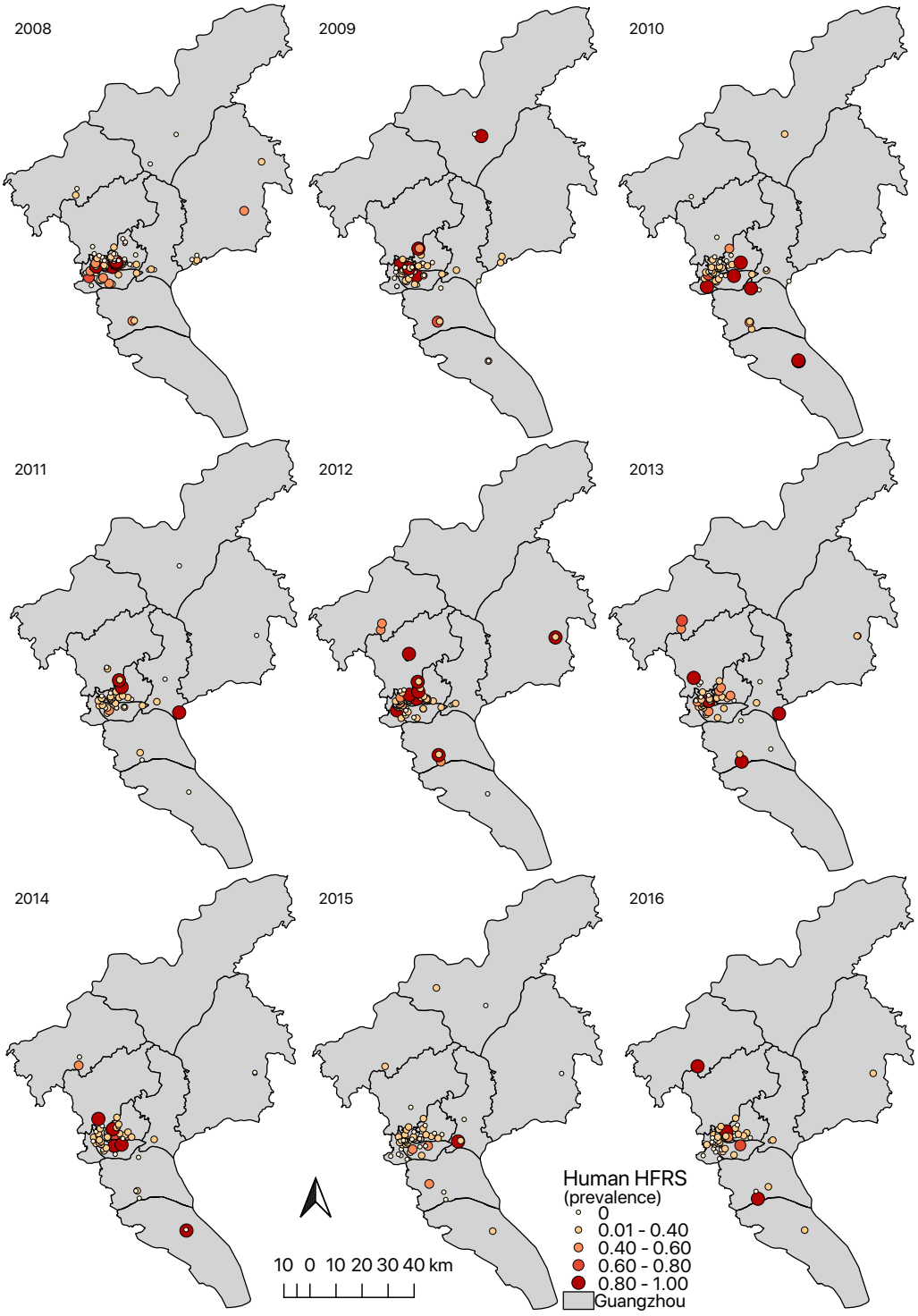

Figure 9. Annual prevalence of Human HFRS for each district in Guangzhou, 2008-2016.

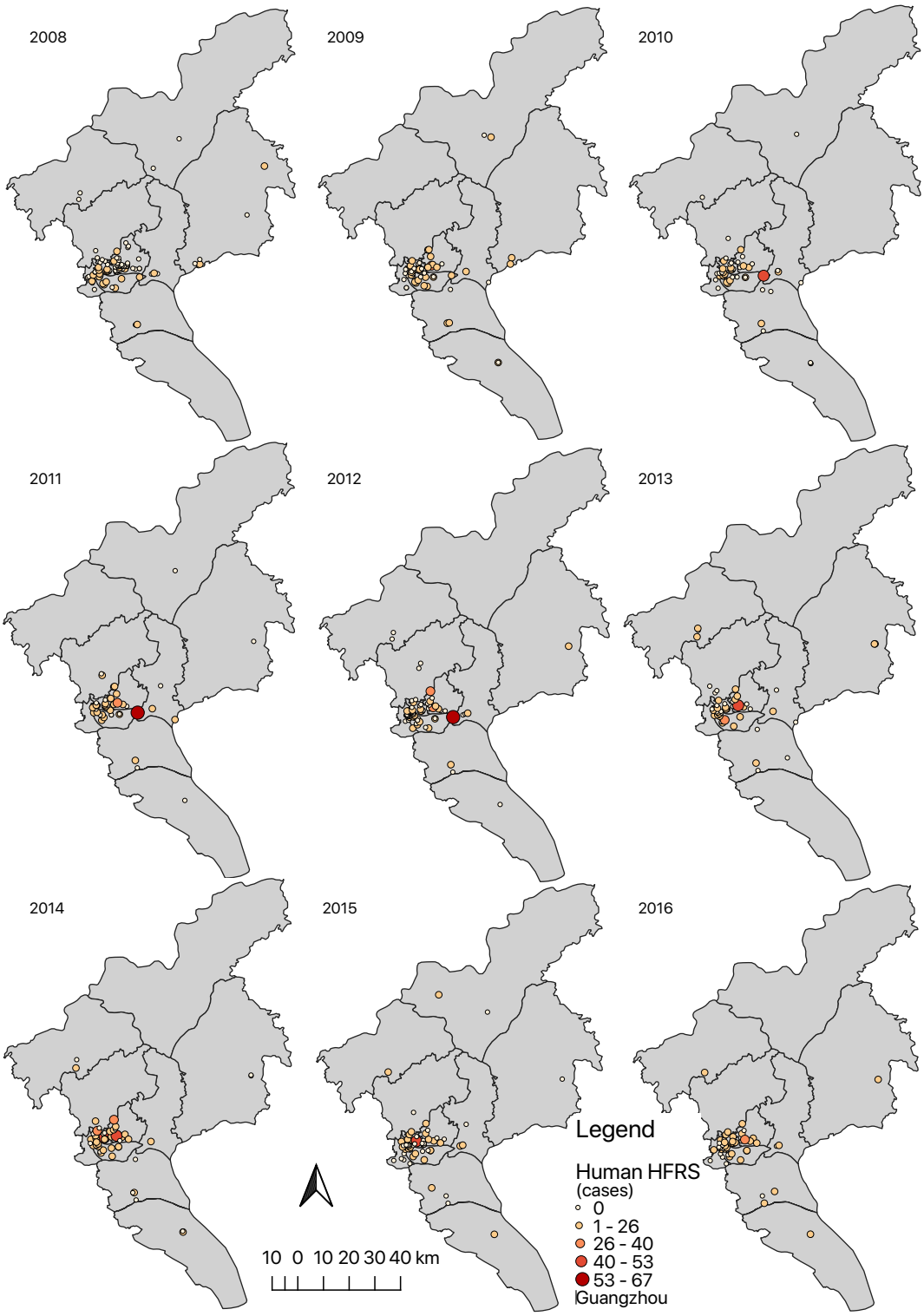

Figure 10. Annual cases of Human HFRS for each district in Guangzhou, 2008-2016.

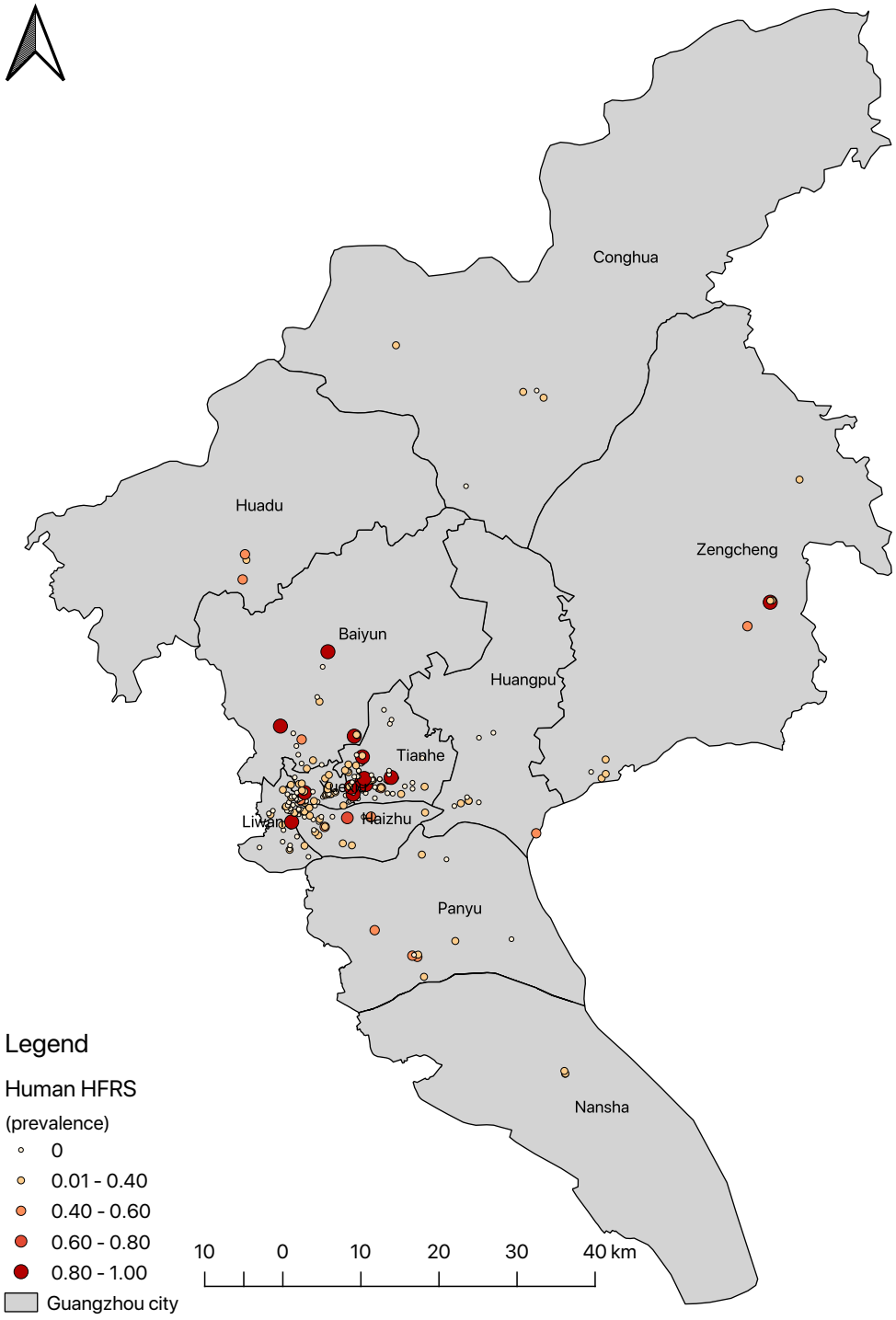

Figure 11. Aggregated prevalence of Human HFRS in Guangzhou, 2008-2016.

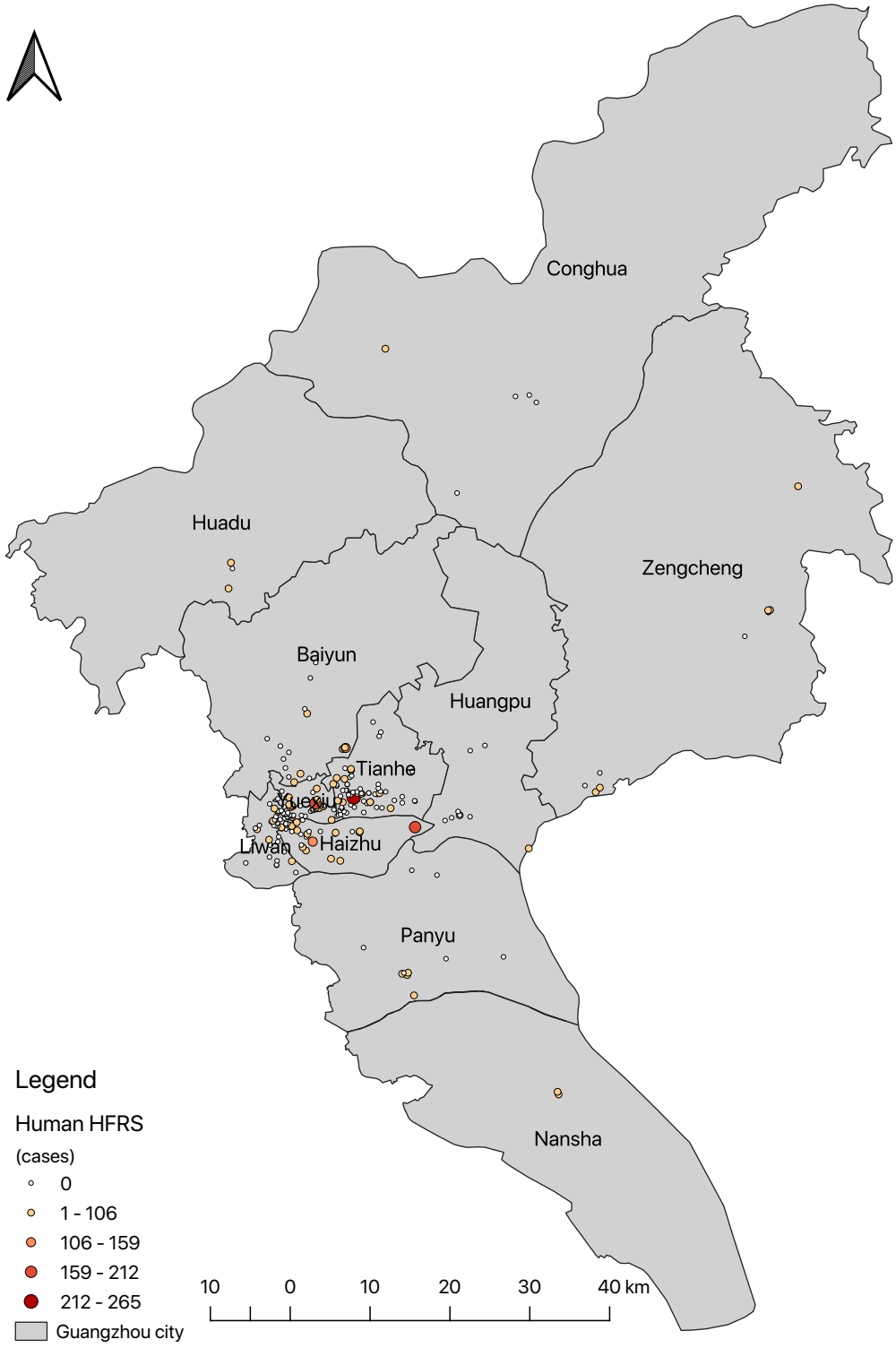

Figure 12. Aggregated cases of Human HFRS in Guangzhou, 2008-2016.

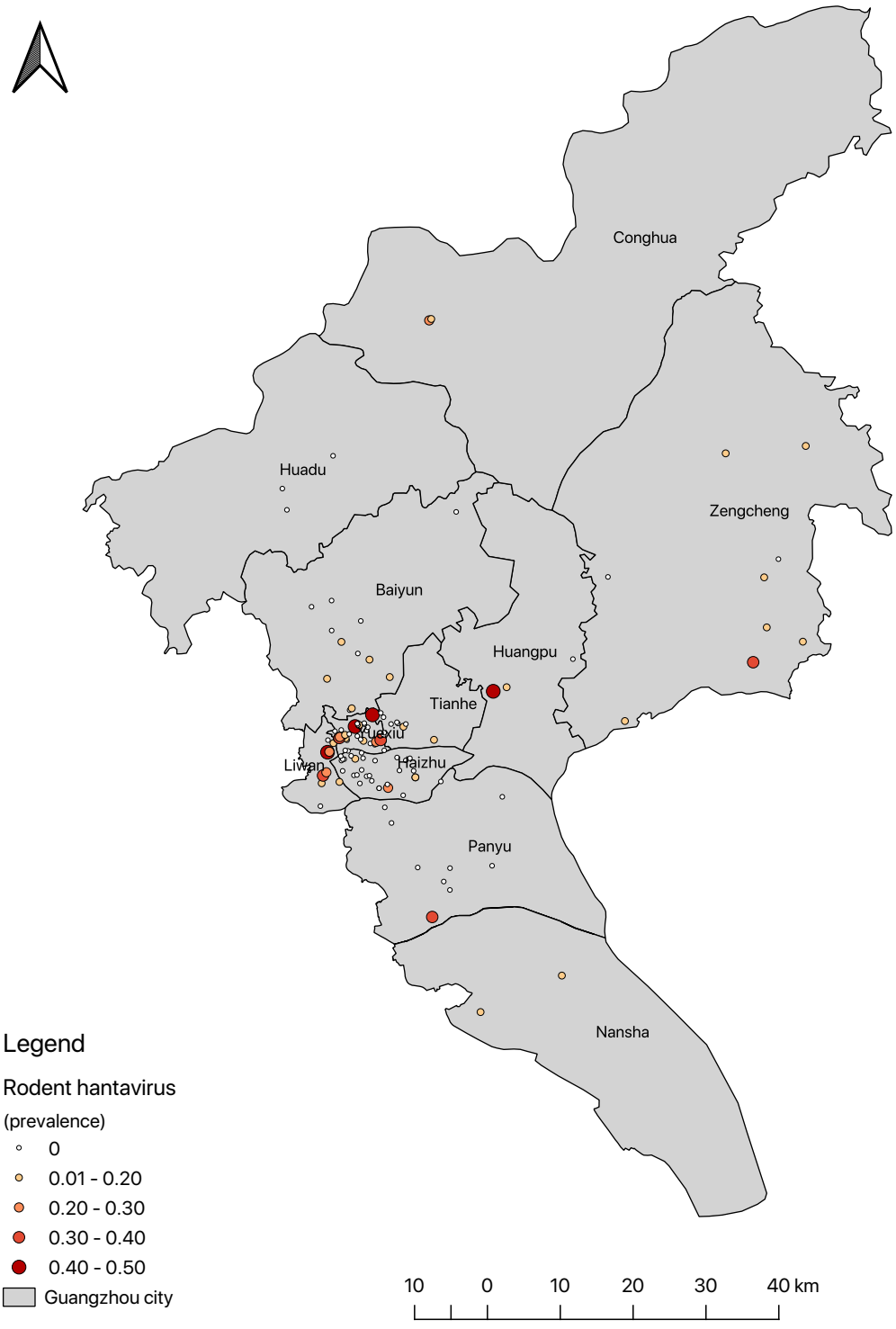

Figure 13. Aggregated prevalence of rodent hantavirus by trap in Guangzhou city (2008-2016).

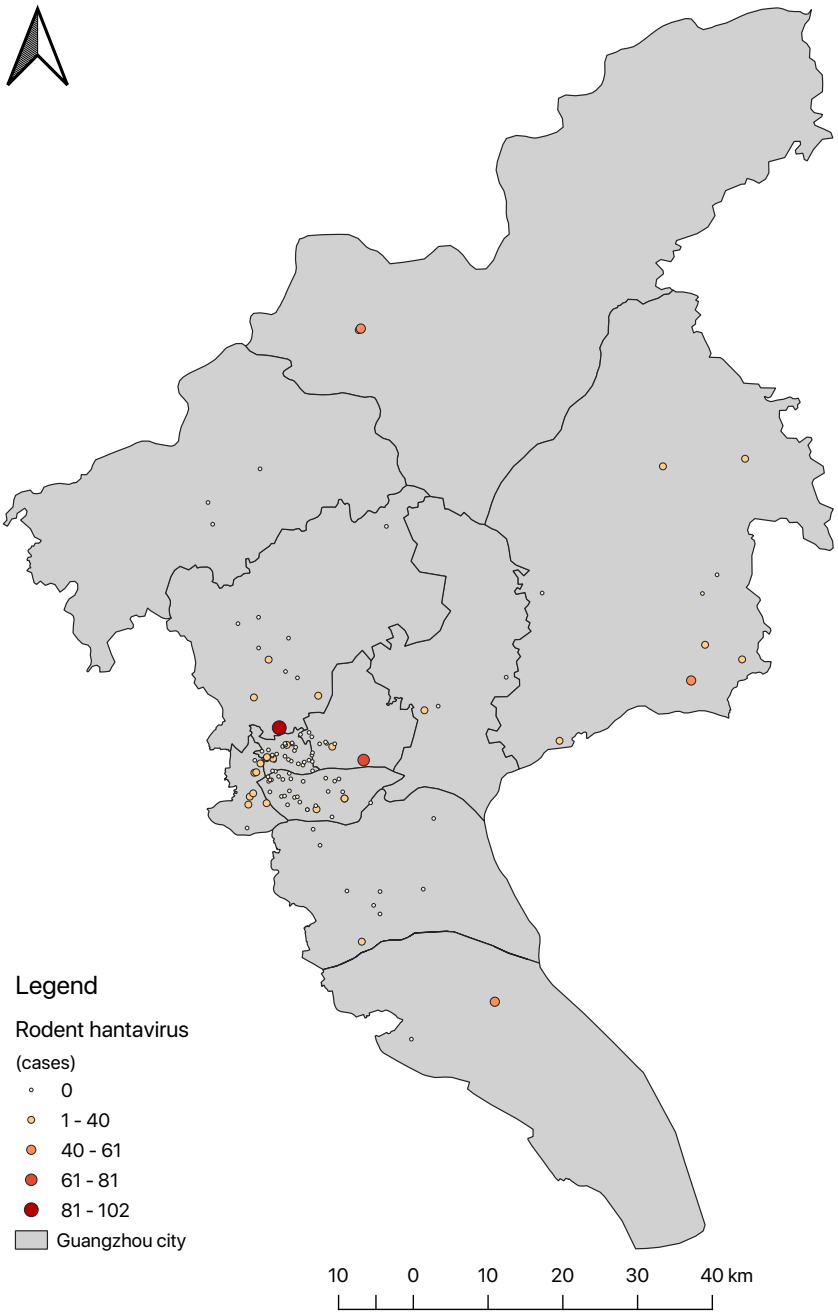

Figure 14. Aggregated cases of rodent hantavirus by trap in Guangzhou city (2008-2016).

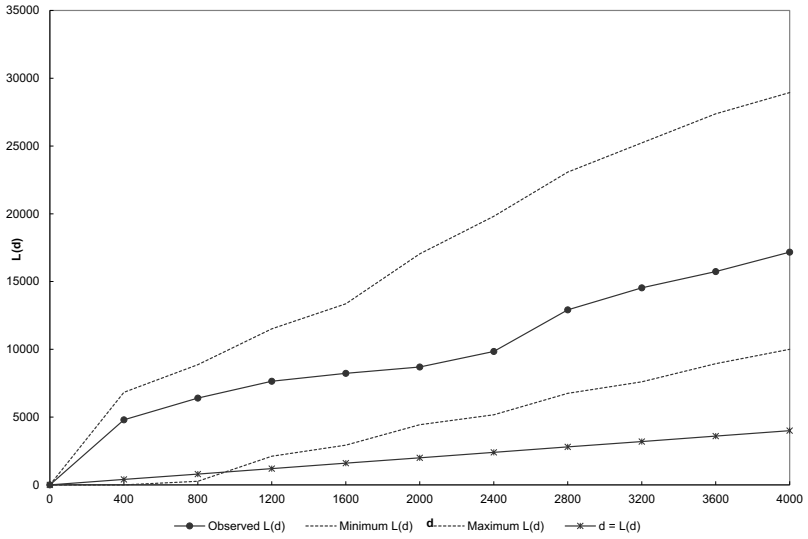

Figure 15. For all of the global weighted-K tests analyzed, all Observed L(d)s fell within the intervals of Minimum L(d)s and Maximum L(d)s like this graph. This indicated all of the points being tested showed a complete spatial random pattern.

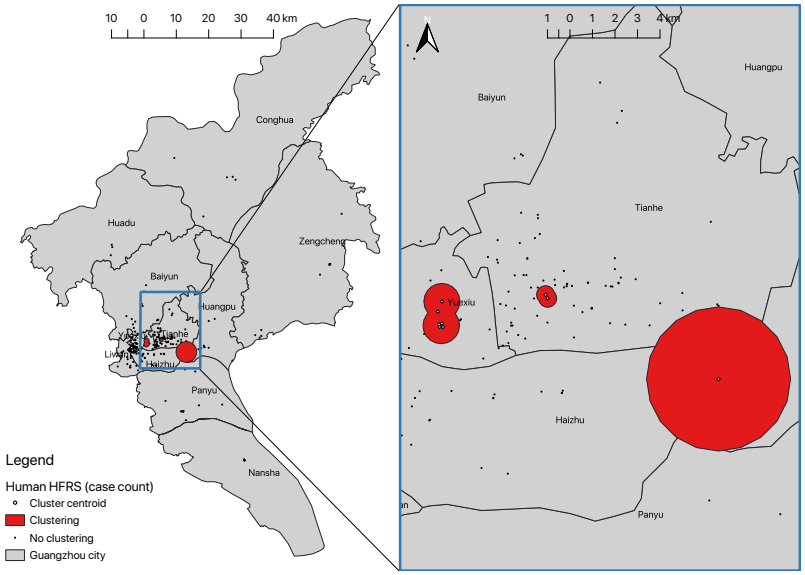

Figure 16. Significant clustering (Gi*[d]> 3.71, P<0.05) of high case count for human HFRS in Guangzhou city between 2008 to 2016.

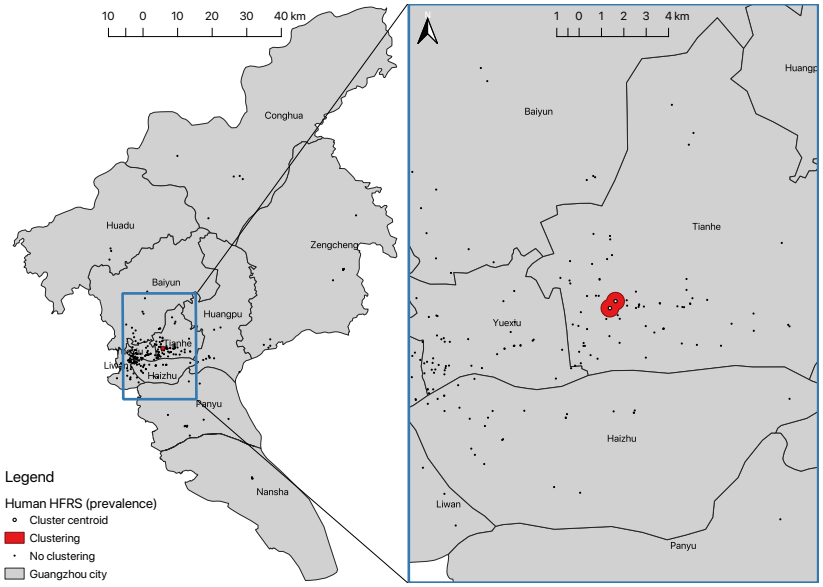

Figure 17. Significant clustering (Gi*[d]> 3.71, P<0.05) of high prevalence for human HFRS in Guangzhou city between 2008 to 2016.

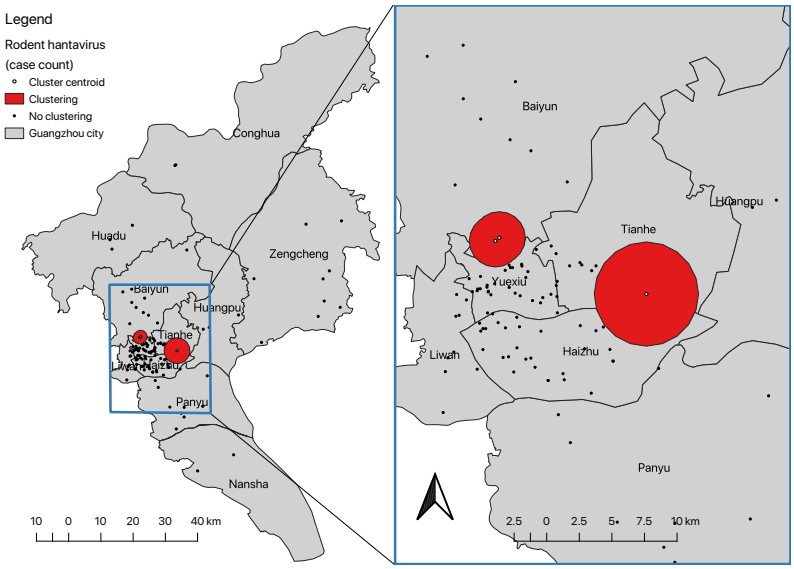

Figure 18. Significant clustering (Gi*[d]> 3.71, P<0.05) of high positive count for rodent hantavirus in Guangzhou city between 2008 to 2016.

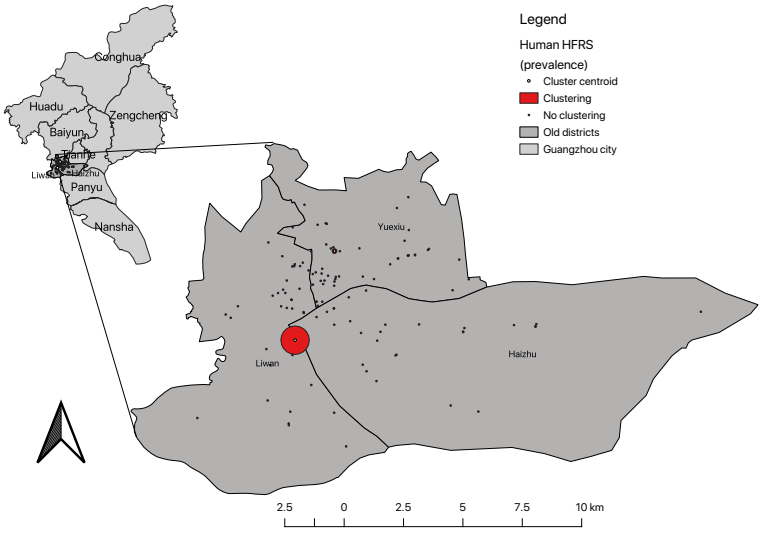

Figure 19. Significant clustering (Gi*[d]> 3.71, P<0.05) of high prevalence of human HFRS in old districts between 2008 to 2016.

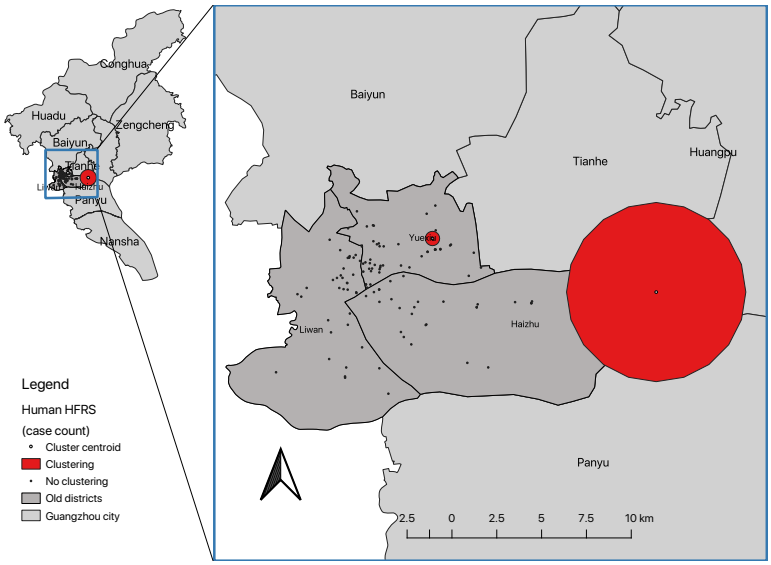

Figure 20. Significant clustering (Gi*[d]> 3.71, P<0.05) of high number of cases of human HFRS in old districts between 2008 to 2016.

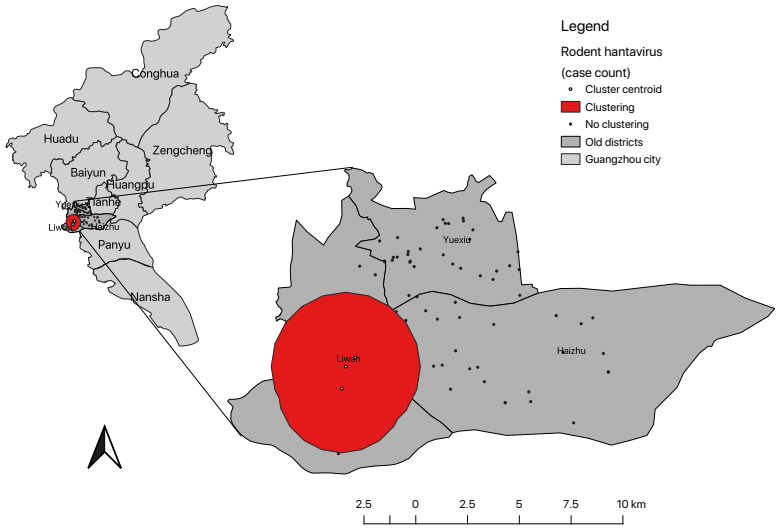

Figure 21. Significant clustering (Gi*[d]> 3.71, P<0.05) of high positive count for rodent hantavirus in old districts between 2008 to 2016.

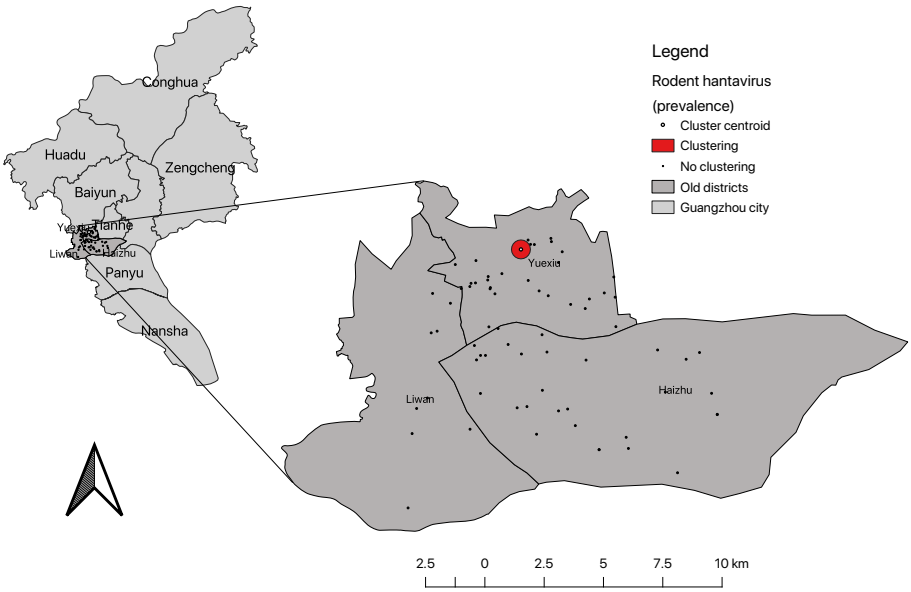

Figure 22. Significant clustering (Gi*[d]> 3.71, P<0.05) of high prevalence for rodent hantavirus in old districts between 2008 to 2016.

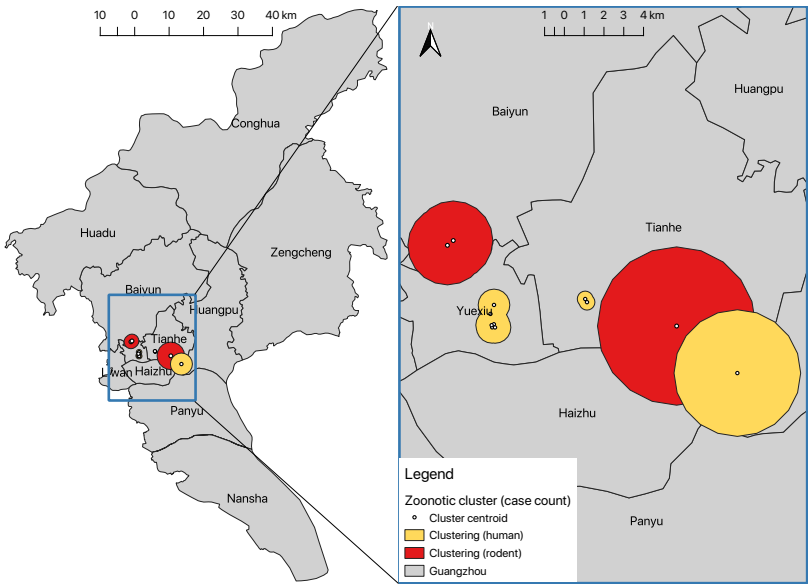

Figure 23. Overlay of significant human HFRS and rodent hantavirus clustering (Gi*[d]> 3.71, P<0.05) of high positive case count in Guangzhou city between 2008 to 2016.

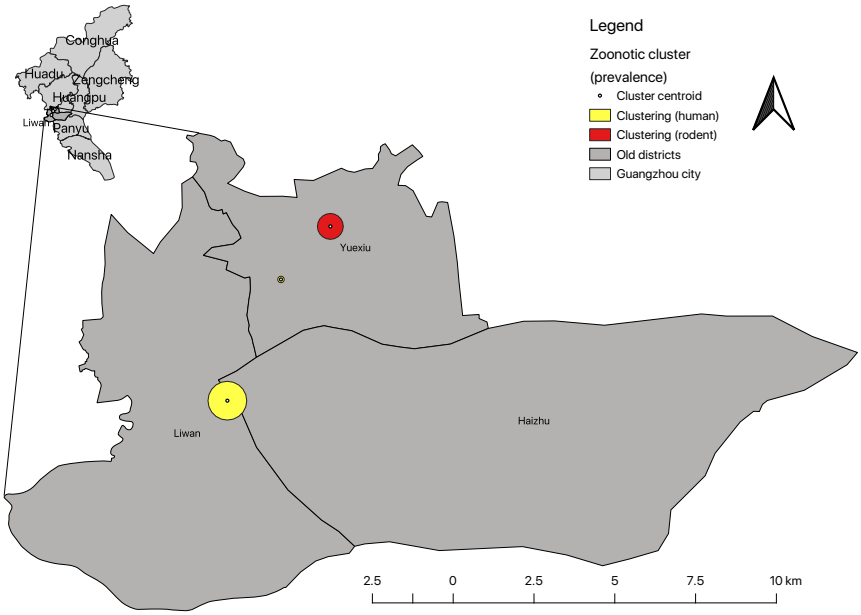

Figure 24. Geographical relationship between significant human HFRS and rodent hantavirus clustering (Gi*[d]> 3.71, P<0.05) of prevalence in old districts between 2008 to 2016.

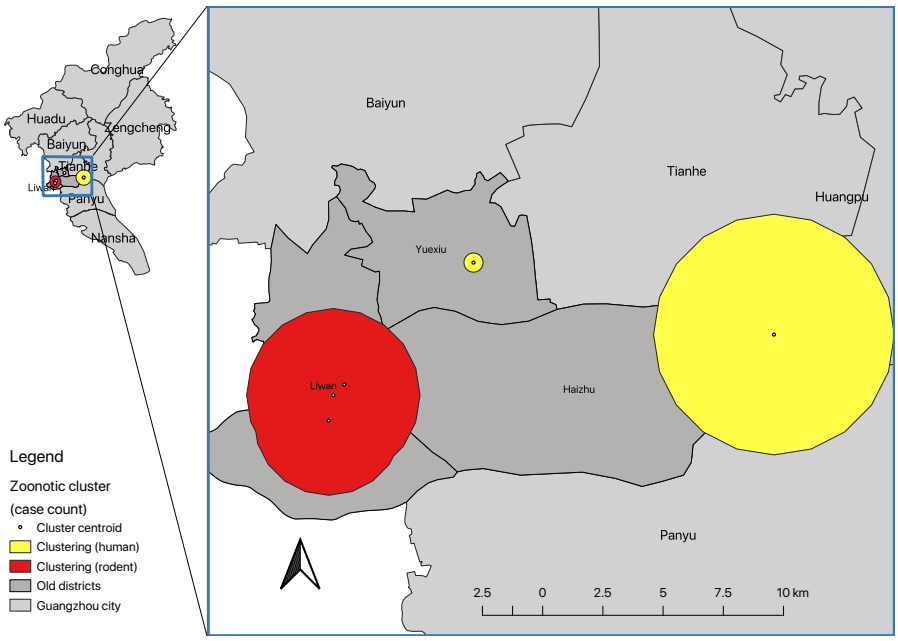

Figure 25. Geographical relationship between significant human HFRS and rodent hantavirus clustering (Gi*[d]> 3.71, P<0.05) of positive case count in old districts between 2008 to 2016.

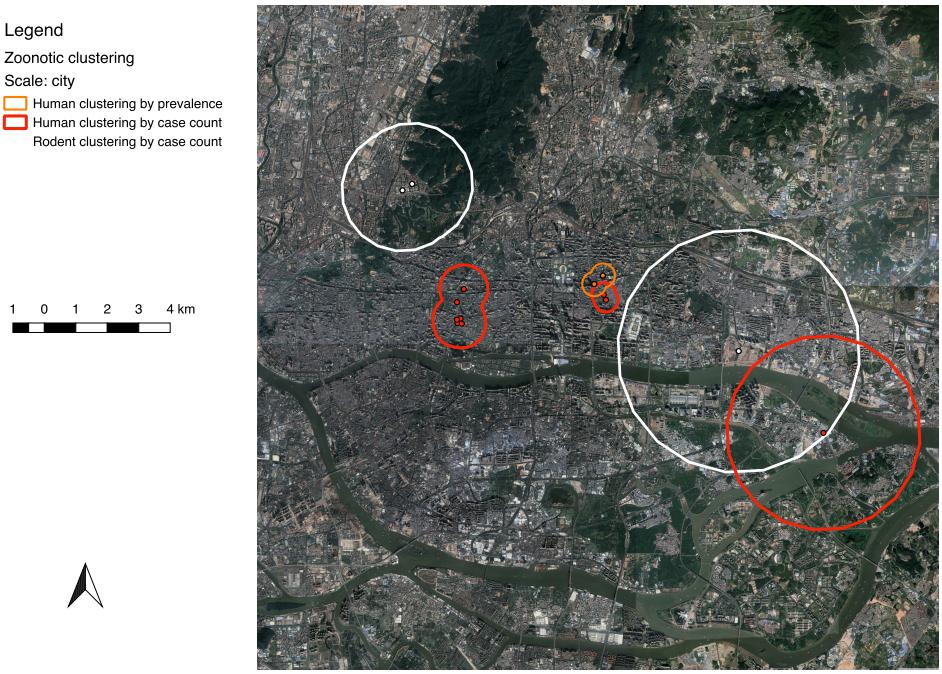

Figure 26. Zoonotic clustering (Gi*[d]> 3.71, P<0.05) in the context of urban environment in Guangzhou city from 2008 to 2016.

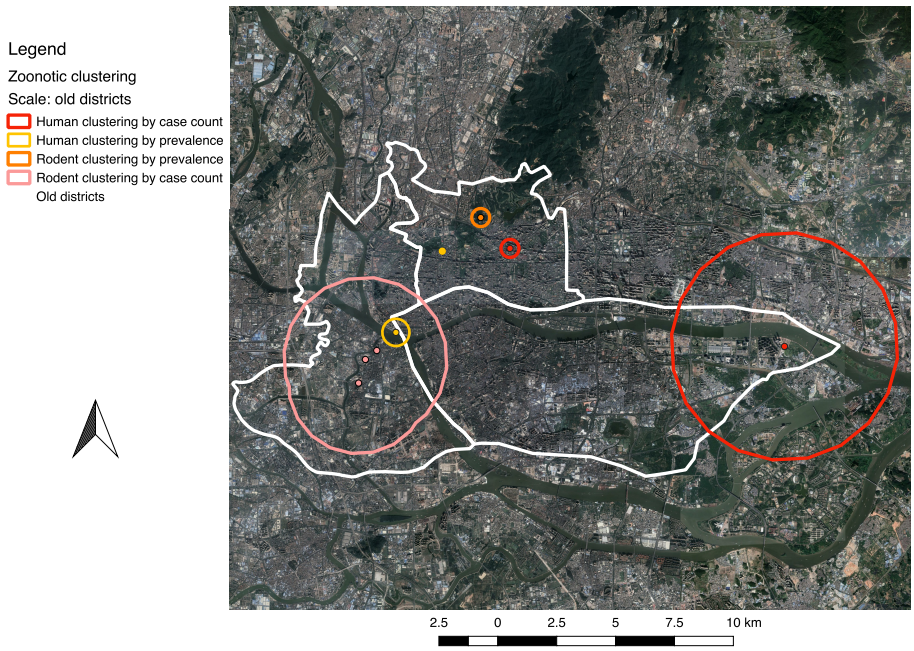

Figure 27. Zoonotic clustering (Gi*[d]> 3.71, P<0.05) in the context of urban environment in old districts from 2008 to 2016.